Journal of Information Systems Engineering and Management
2025, 10(3)
e-ISSN: 2468-4376
https://www.jisem-journal.com/

Research Article

Enhanced Lung Cancer Diagnosis via Attention-based Deep Belief Network segmentation and GWO-EHO Based Deep Learning Classification

Dr. P. Gomathi
[1] *Professor in Electronics and Communication Engineering, Study World College of Engineering, Coimbatore*

ARTICLE INFO

Received: 12 Nov 2024

Revised: 20 Dec 2024

Accepted: 19 Jan 2025

ABSTRACT

Lung cancer is the biggest contributor to cancer-related deaths around the world, and early identification is critical to improving patient outcomes. Nonetheless, early cancer detection is a significant difficulty, especially in low-resource areas where access to healthcare facilities and skilled radiologists is limited. The input CT lung cancer images are collected from DICOM file format dataset. To reduce noise in the resulting dataset, pre-processing is conducted to the images. A Adaptive optimum weighted mean filter (AOWMF) is applied for the pre-processing phase. The Attention-based Deep Belief Network (ADBN) segmentation approach is used to process the segmentation and determine the afflicted area of the lung cancer. Utilizing the DenseNet-201 Model, the feature is extracted. The proposed research uses the Grey Wolf Optimization based Elephant Herding Optimization (GWO-EHO) architecture to classify brain cancer as normal, benign and malignant". The proposed EHO model offers improved precision and a better rate of brain tumor classifies with a high accuracy..

Keywords: CT scan, AOWMF, GWO-EHO algorithm, DenseNet-201 Model, ADBN segmentation.

INTRODUCTION

Lung cancer is a serious, sometimes fatal disease caused by the uncontrolled growth of abnormal cells in the lungs. It is one of the leading causes of cancer-related deaths worldwide, owing to its penchant for being discovered at an advanced stage. The two main types of lung cancer are cancer of the non-small cells (NSCLC), which accounts for a great deal of cases, and lung cancer with small cells (SCLC), that is more dangerous and spreads quickly. Common risk factors include exposure to secondhand smoke, air pollution, chronic smoking, and job-based exposure to toxins like asbestos. Deep learning models, particularly convolutional neural networks, are often used to interpret medical imaging data, such as CT scans and chest X-rays. These algorithms can automatically learn and extract complex patterns and features in images that humans may find difficult to detect. Lung cancer is the leading cause of cancer-related death globally. Patients with localized cancer had a 60% 5-year survival rate compared to 6% for those with metastatic disease when early identification is achieved [1]. This work provides a new way to detect lung cancer that combines watershed segmentation techniques with Gabor filters to address the drawbacks of prior approaches [2]. Using a novel digital image processing method, CT (Computerized Tomography) images from patients with lung cancer are analyzed [3]. Several strategies have been developed to increase cancer detection efficiency [4]. A deep neural network is created and evaluated to identify lung cancer with a high degree of precision. The suggested technique has 99.269% accuracy, 99.1251% specificity, and 99.1121% sensitivity. The complete simulation is carried out in MATLAB [5].

Contribution of this Work

According to the analysis of the research objective, a CT scan will be used to classify lung cancer in the following areas:

1. Implementation of the AOWMF for effective noise reduction in CT lung cancer images during the pre-processing stage.

Journal of Information Systems Engineering and Management
2025, 10(3)
e-ISSN: 2468-4376
https://www.jisem-journal.com/

Research Article

2. Use of the ADBN for precise segmentation of the affected lung regions, enhancing the identification of cancerous areas.
3. Application of the DenseNet-201 deep learning model to extract meaningful and high-quality features from segmented lung images.
4. Development of a hybrid GWO-EHO model for highly accurate classification of lung cancer into normal, benign, and malignant categories.

The proposed system's structure will be covered in the part that follows: Section 1 presents the introduction and two related works on lung cancer. Section 3 defines the system that is suggested. Section 4 analyses the findings and calculates performance values. The conclusion and future work is explained in Section 5.

1. Related Work

Chen et al. [6] have proposed, the classification of lung nodules is critical for diagnosing lung cancer and improving patient survival. LDNNET uses the LUng Nodule Analysis 2016 (LUNA16) database to classify lung nodules and the KAGGLE DATA-SCIENCE-BOWL-2017 (Kaggle DSB 2017) database to classify lung cancers. Da et al. [7] have suggested, a Lung cancer was responsible for 26% of all malignancy-related fatalities, representing more than 1.5 million worldwide. The proposed method investigates the performance of deep learning using transfer learning for lung nodular malignancy classification. Nazir et al.[8] have recommended, Using lung CT image LIDC-IDRI, the effectiveness of the idea put forward was evaluated. The Cancer Imaging Archive (TCIA) hosts the LIDC, which is publically available on their website. This dataset was developed in collaboration with seven academic centers and eight medical imaging organizations.

Das et al. [9] have described, a concentrate on individual imaging modalities for the identification of lung cancer; no particular methods have been found for PET and CT images separately to achieve efficient and noise-free hybrid imaging for the detection of lung cancer. According to the survey, multiple picture preprocessing filters are utilized for various types of noise. Gainey et al. [10] have discussed, to create a model for predicting non-small cell lung cancer (NSCLC) survival outcomes following stereotactic body radiation treatment (SBRT) using deep-learning segmentation-based prognostication (DESEP). Training of the DESEP model involved imaging 108 NSCLC patients with different phases of disease and treatment histories.

Finnegan et al. [11] have reported, these same patient picture sets were used to autonomously segment the heart employing a leave-one-out technique, while the remaining 18 patients were used as an atlas set. When comparing automatic segmentation to hand contouring, the consistency of the former was evaluated using the Dice similarity coefficient (DSC) and mean absolute surface-to-surface distance (MASD). Sun et al. [12] have proposed, four radiologists' annotations were used to segment the nodules, and each slice of nodule images was rotated to create 13,668 samples. Convolutional neural networks (CNN), deep belief networks (DBN), and stacking denoising autoencoders are three multichannel ROI-based deep structured algorithms that were created and put into practice in this study. For contrast, we built a CADx system with hand-crafted aspects like density, texture, and morphological qualities.

Hussain et al. [13] have proposed, the results for separating non-small-cell lung cancer (NSCLC) from small-cell lung cancer (SCLC) were statistically significant when morphological, textural, and elliptic Fourier descriptors (EFDs) were extracted. The most significant findings based on textural features, when using MFE with deviation from the mean, produce a P-value of 1.95E-50. Nanglia et al. [14] have reported, the approach for lung cancer classification, lobe segmentation, and candidate nodule extraction yielded encouraging outcomes using the publicly available LUAN16 dataset. For the classification of lung cancer, the enhanced AlexNet-SVM model exhibits 97.70% F1, 98.84% sensitivity, 97.47% specificity, 97.53% precision, and 97.98% accuracy. Rodrigues et al. [15] have discussed, it received an accuracy and F-Score of 96.7% and 53.2%, respectively, for the first job and 74.5% and 53.2%, respectively, for the second. These test findings imply that the SCM was able to extract certain features of the tumors from the pictures, and as a result, it might be seen as a useful tool to help doctors diagnose lung nodule cancer more precisely.

PROPOSED SYSTEM

Figure 1 depicts a comprehensive system for classifying medical images, specifically lung imaging, into three categories: normal, benign, and malignant [16]. The procedure starts with the input image, which is preprocessed using the AOWMF to improve image quality and remove noise. The preprocessed image is then transferred to the ADBN model for segmentation, which isolates and identifies regions of interest in the image.

Journal of Information Systems Engineering and Management
2025, 10(3)
e-ISSN: 2468-4376
https://www.jisem-journal.com/

Research Article

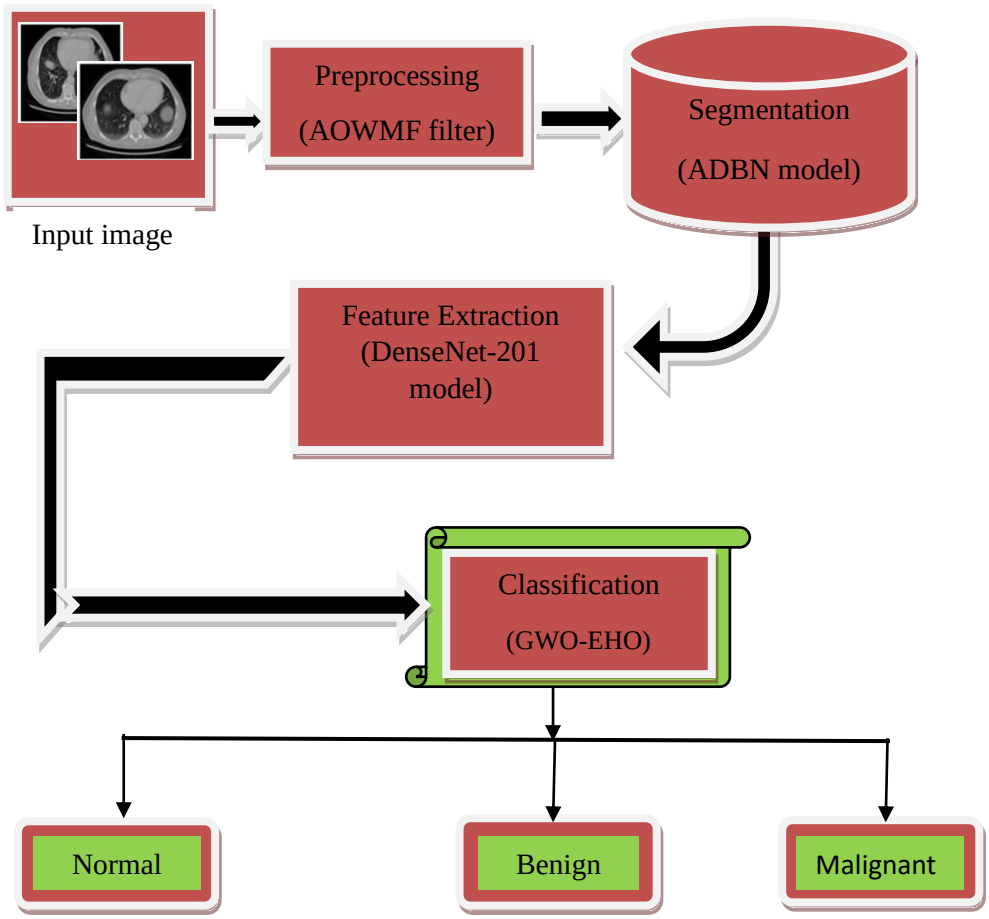

Fig 1: Block diagram for GWO-EHO based lung cancer Classification

The DenseNet-201 model, a deep convolutional neural network noted for its ability to extract detailed characteristics from medical pictures, is then used. The retrieved features are then transferred to the classification module, which employs a hybrid approach using GWO-based EHO deep learning algorithms to improve accuracy and performance. Finally, based on the classification results, the image is categorized as Normal, Benign, or Malignant, aiding in effective diagnosis and decision-making.

1.1. Adaptive optimum weighted mean filter (AOWMF)

Unlike the regular mean filter, which eliminates low levels of rician noise with a constant window size, the adaptive weighted mean filter decreases excessive noise, which drastically affects the clarity of MR images, by varying the window size. With the adaptive weighted mean filter, the window size is progressively increased to match the highest and lowest pixel values of two consecutive windows. If the value of the window's center pixel is either the lowest or the highest, the window's average weighted value is restored. The intensity value stays the same if the value of the central pixel is neither the lowest nor the highest. $x_{i,j}$ is the center pixel intensity value M×N (x,y) of the coordinate system for the original image of size. When $[\![DR_{min} \leq xi,j \leq DR_{max}.$ ", that is the dynamic range (DR). The letter *"dr"* stands for a distorted image. In order to replace an invalid pixel in an image, utilize the dynamic ranges DR_{min} and DR_{max}found in eqn (7).

$$dr_{i,j} = \begin{cases} DR_{min} & withP_a \\ DR_{max} & withP_b \\ x_{i,j} & withP_{1-a-b} \end{cases} \quad (1)$$

Where, $noise = a + b$, a and b are expressed as the probability that a certain pixel will be twisted as a result of the effects of $P\ maximum$ (speckle) and $P\ lowest$ (Rician) noise.

1.2. Segmentation using ADBN

The second stage, segmentation, entails taking an enhanced image and extracting the region that is impacted. ADBN is used for segmentation in this investigation since it processes images on several levels. Furthermore, the computer network contains a vast quantity of data acquired from earlier study, which aids in accurately

Journal of Information Systems Engineering and Management
2025, 10(3)
e-ISSN: 2468-4376
https://www.jisem-journal.com/

Research Article

locating the issue location while using the minimum estimation time. The calculation of data probability is more significantly impacted by this segmentation network. The DBN employs a multi-layered restricted Boltzmann machine (RBM) [17]. By employing the RBM operating concept, one can comprehend the operational mode of DBN. The visible and hidden layers in the RBM deep learning system are represented by VL and HL, respectively. There is no connection between the visible and hidden levels. The DBNs have taken the following specific actions:

First Step: A thorough distribution of probabilities of the visible (VL) and hidden layers (HL).

Second step: *I* stands for the visible layer range and j for the hidden layer range, which are used to convert the RBM data from the visible layer to the hidden layer..

Third step: It is possible to use the Boltzmann probability for identifying the setup's joint range of probabilities.

Fourth step: To obtain the partition function, the sum of all possible visible and hidden vector pairs is used.

Fifth step: To determine the activation conditional probability, the logistic functions employ the VL and HL.

1.3. DenseNet-201 based Feature Extraction

Feature extraction is the process of converting original data into mathematical characteristics while retaining the dataset's content. It performs better after feature extraction than whenever the raw data is fed straight into the algorithm. Lung CT segmented images are subjected to feature extraction using DenseNet-201. DenseNet-201 is a DL transfer learning technique that solves present problems by drawing on past problems [18]. The DenseNet-201 technique is applied to lower and high dense blocks, which are separated into four phases according to the number of layers in each block, in order to extract the characteristics of the BraTS 2020 dataset. The five features that DenseNet201 retrieves are inverse difference moment (IDM), variance, contrast, correlation, and entropy. DenseNet-201 is configured with the following parameters: *20.0*, depth *201,* and size *77MB*. A high success rate for the following steps is ensured by recovering the textual features from segmented images. Eqn 8 evaluates the features employed in this investigation.

(a)Contrast

$$f_1 = \sum_{n=0}^{N_{g-1}} n^2 \sum_{i=1}^{N_g} \sum_{j=1}^{N_g} p(i,j) \quad (2)$$

Where, N_g shows a significant amount of gray levels in the actual image.

(b)Correlation

The correlation characteristic indicates the linear dependence of the gray levels on nearby pixels. Eqn 3 represents correlation, which is a statistical measure of the relationship between two variables,

$$f_2 = \frac{\sum_i \sum_j (i,j) p(i,j) - \mu_x \mu_y}{\sigma_x \sigma_y} \quad (3)$$

Where μ_x, μ_y, $\sigma_{x,} \sigma_y$ are the input image's mean and standard deviation, arranged in rows and columns.

(c)Variance

Variance is an indication that indicates how values differ from the mean. The measurement of the degree to which grayscale values are dispersed throughout the input image is known as variance, and Eqn 4 illustrates this.,

$$f_3 = \sum_i \sum_j (i-\mu)^2 p(i,j) \quad (4)$$

Where μ reflects the average of all images.

(d)Entropy

Entropy denotes the distribution of grey-level randomness. Entropy should be large when the image's gray levels are distributed randomly, as demonstrated by Eqn 5.

$$\boldsymbol{f_4} = \sum_i \sum_j p(i,j) log(p(i,j)) \quad (5)$$

IDM

IDM denotes image smoothness information. Eqn 6 computes IDM, which is predicted to be big when the gray scale of the pixels are the same.

$$f_5 = \sum_i \sum_j \frac{1}{1+(i-j)^2} p(i,j) \quad (6)$$

Journal of Information Systems Engineering and Management
2025, 10(3)
e-ISSN: 2468-4376
https://www.jisem-journal.com/

Research Article

Usually used for lung CT image classification, the features are given as input so that they can be selected and then classified.

1.4. GWO-EHO based Classification

A novel hybrid algorithm that blends the characteristics of the GWO based EHO algorithms is described in this section. As mentioned earlier, the GWO algorithm makes use of wolves' hierarchical structure and hunting habits. However, the creation of optimization algorithms has been inspired by the existence of an elephant clan, where each clan's members are subordinate to the leader and male elephants are kept apart from the group [18]. The hybrid GWO-EHO algorithm groups wolves based on elephant clan life, dividing them into a set number of clans each. After determining the α, β and γ wolves for each clan, the GWO algorithm's proposed relationships are utilized to design the process of upgrading the wolves' condition. Alpha, beta, and gamma wolves are included in the text along with the current status of α wolves in each clan. A new separation operation then outlines the process. One or two of the proposed new operator's wolf clans are picked at random, and the most undesirable wolves in each of these clans are replaced using the algorithm below.

$$x_{worst,ci} = t \times (x_{max}) \times (-1)^{cindex} \quad (7)$$

The value of the variable t from the following equation is lowered linearly using Eqn 8 and proportionate to Max_{iter} as it goes from one to zero.

$$t = 1 - Iter(\frac{2}{Max_{iter}}) \quad (8)$$

$$Iter \in [0, \frac{Max_{iter}}{2}) \quad (9)$$

In the relationship above, the current counter $iter$ Max_{iter} is equal to the algorithm's maximum repetition cycle, and the top bound of the wolves, denoted by X_{max}, will be $Cindex = 1$ or $cindex = 2$. In the proposed GWO-EHO algorithm, the top three best answers for mathematical modeling were kept, and other agents were encouraged to modify their opinions in response to the remaining three solutions. In this regard, the subsequent formulas are recommended:

$$\left|-\overrightarrow{X}\overrightarrow{X_\delta} \cdot \overrightarrow{C_3}\right| = \overrightarrow{D_\delta}, \left|-\overrightarrow{X}\overrightarrow{X_B} \cdot \overrightarrow{C_2}\right| = \overrightarrow{D_B}, \left|-\overrightarrow{X}\overrightarrow{X_\alpha} \cdot \overrightarrow{C_1}\right| = \overrightarrow{D_\alpha} \quad (10)$$

$$\overrightarrow{-A_3} \cdot \overrightarrow{D_\delta}\,\overrightarrow{X_\delta} = \overrightarrow{X_3}, \overrightarrow{-A_2} \cdot \overrightarrow{D_B}\,\overrightarrow{X_B} = \overrightarrow{X_2}, \overrightarrow{-A_1} \cdot \overrightarrow{D_\alpha}\,\overrightarrow{X_\alpha} = \overrightarrow{X_1} \quad (11)$$

$$\left(\vec{X}(t+1) = \frac{\overrightarrow{X_1}+\overrightarrow{X_1}+\overrightarrow{X_1}}{3}\right. \quad (12)$$

The second and third-best solutions are known as beta (β) and delta (δ), respectively, as alpha (α) is considered the best alternative [19]. The remaining probable solutions are referred to as omega (ω). The gray wolves attack when the prey stops moving, as mentioned earlier. Reduce the value of $\vec{a}$ to imitate approaching the prey. $\vec{A}$ is dependant on another $\vec{a}$. The future positioning of an explore agents can be somewhere between its present position and the prey's location when random values of $\vec{A}$ fall within the interval $[-1,1]$. The matriarch of clan ci controls the next location of every elephant in the clan because all tribes are influenced by her. One way to update the elephant j in clan ci is by means of,

$$X_{new,ci,j} = X_{ci,j} + \alpha \times (X_{best,ci} - X_{ci,j}) \times r \quad (13)$$

Where, $X_{new,ci,j}$ and $X_{ci,j}$ are, respectively, the original location for elephant j in clan ci and the recently updated location. The scale factor $\alpha \in [0,1]$ determines how much ci affects $X_{ci,j}$. $(X_{best,ci})$ shows matriarch ci, the best elephant person in clan $ci.r \in [0,1]$. Figure 2 displays the flowchart for the GWO-EHO algorithm.

Journal of Information Systems Engineering and Management
2025, 10(3)
e-ISSN: 2468-4376
https://www.jisem-journal.com/

Research Article

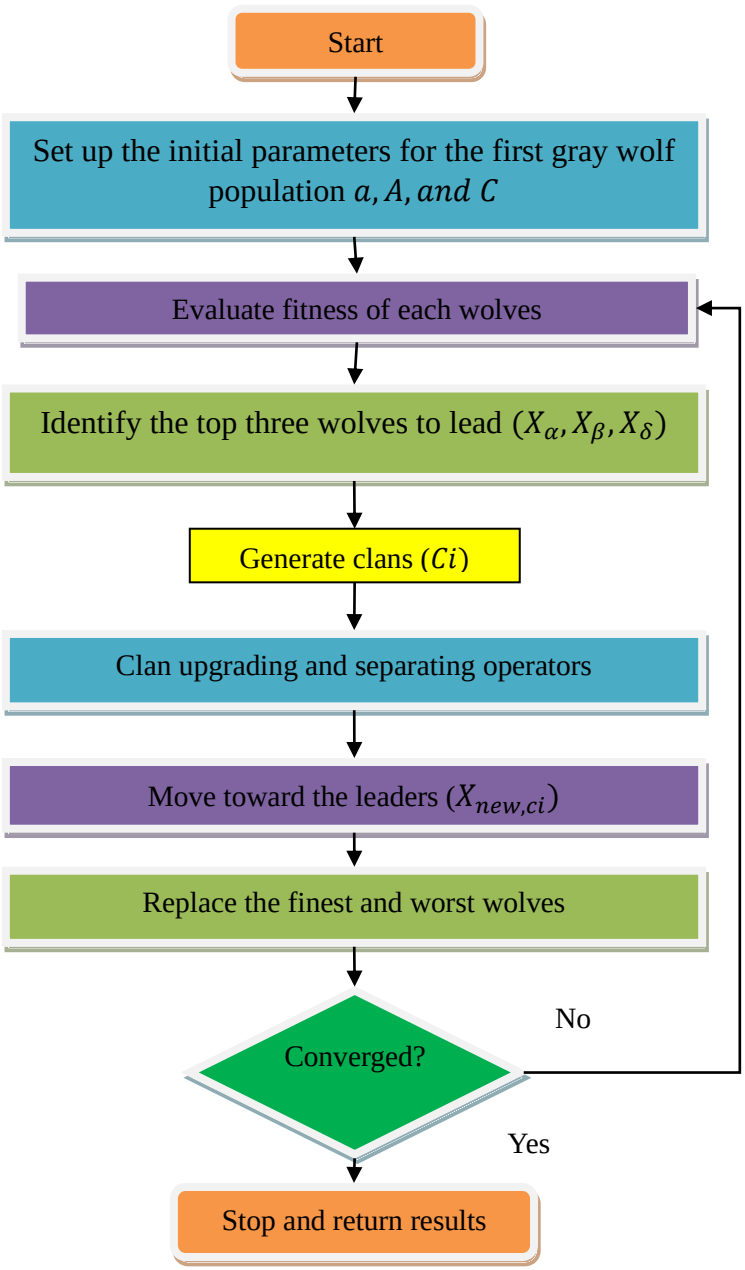

Fig 2: Flowchart for GWO-EHO algorithm

Algorithm 1: Pseudocode for GWO-EHO algorithm

Begin
Initialization
for $ci = 1$ to $nClan$ (for the entire wolf population's clans)
for j =1 to nci (for every wolf in the clan ci)
Produce $X_{new,ci}$ and update $X_{ci,j}$ in compliance with GWOEHO by Eqn. (10), (11), (12)
if $X_{ci,j} = (X_{best,ci})$ then
Update $X_{ci,j}$ and produce $X_{new,ci,j}$ by Eq. (13)
end if
end for j

Journal of Information Systems Engineering and Management
2025, 10(3)
e-ISSN: 2468-4376
https://www.jisem-journal.com/

Research Article

end for *ci*
End

1.5. Performance evaluation of classification results

The Confusion matrix is one of the most significant values in deep learning networks' classification method. The Confusion matrix provides the rest of the values.

$$\text{Accuracy} = \frac{\text{TP}}{\text{TP+TN+FP+FN}} \quad (14)$$

$$\text{Sensitivity} = \frac{\text{TP}}{\text{TP+TN}} \quad (15)$$

$$\text{Specificity} = \frac{TN}{TN+FP} \quad (16)$$

$$\text{Precision} = \frac{\text{TP}}{\text{TP+FP}} \quad (17)$$

2. Result and Discussion

Conduct thorough research employing chest CT pictures as a testing platform to see whether they were associated with normal or lung cancer patients. The datasets, performance metrics, model hyper- Parameters findings, and effectiveness comparisons are all covered in this part.

2.1. Dataset

In the DICOM file format, the data was recorded with particular tags for imaging, research dates, birth dates, and other details. The imaging modalities used was CT, PT, DX, and CR. 2791 photographs from various patients were used for evaluating lung cancer. An assortment of DICOM-formatted CT scan images. Table 1 displays each image for lung cancer classification.

Table 1: Total images for lung cancer classification.

Normal	Benign	Malignant
2285	5	1
1	229	0
1	42	227

2.2. Input images

Cancer diagnosis is one of the most difficult difficulties that engineers face today. Because recognition is a heterogeneous process that appears to be dependent on a variety of variables, an appropriate model has yet to be developed despite much research.

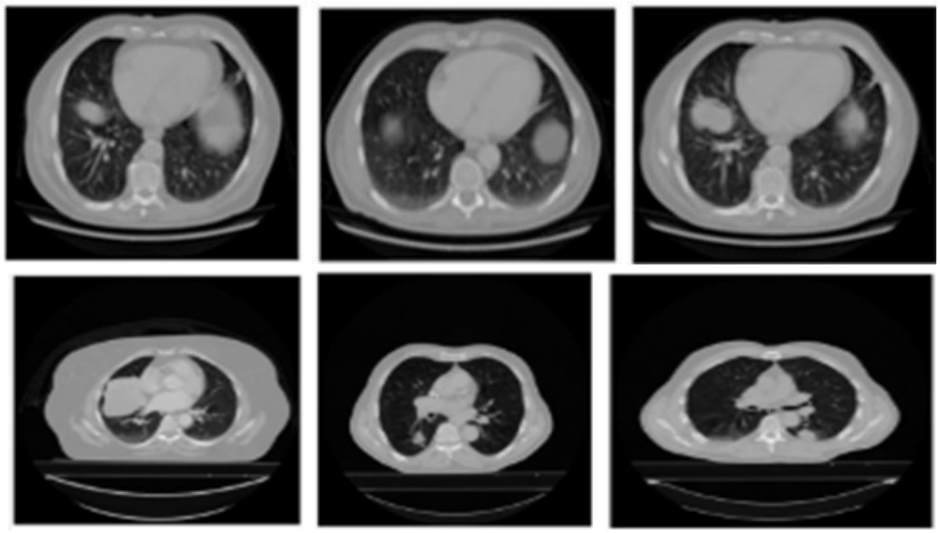

Fig 3: Input images

Journal of Information Systems Engineering and Management
2025, 10(3)
e-ISSN: 2468-4376
https://www.jisem-journal.com/

Research Article

Several studies were conducted to increase the precision of cancer identification approaches. This study established a novel system for detecting early cancer that is more accurate, precise, and simple to calculate. This study creates a GWO-EHO model for accurate liver disease prediction. Figure 3 depicts the sample input image in CT scan.

2.3. Pre-processing image

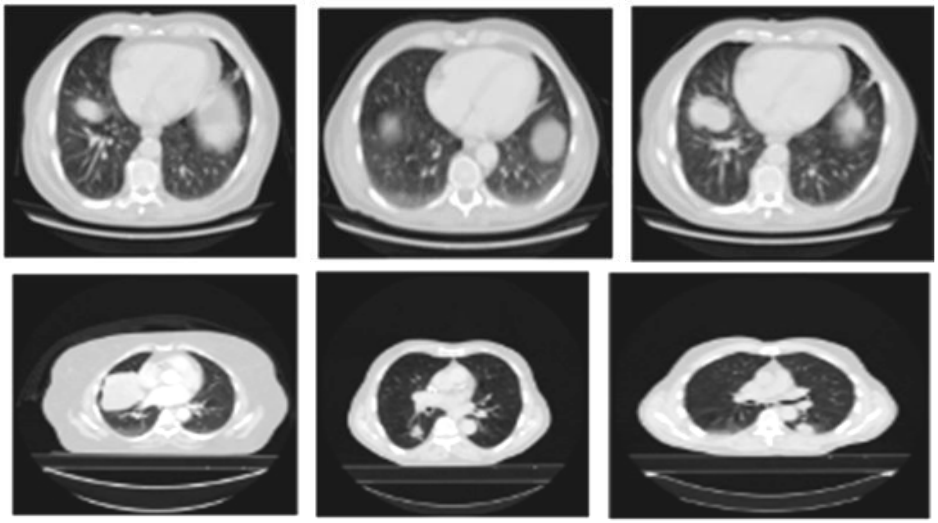

Fig 4: Preprocessed images by using AOWMF filter

Figure 4 illustrates how the suggested method preprocesses liver tumor CT images using a AOWMF filter. The filter, shown here, smoothes and sharpens the image edges. When pretreatment procedures are utilized, the image's pixel quality increases and is then segmented.

2.4. Segmented lung cancer image

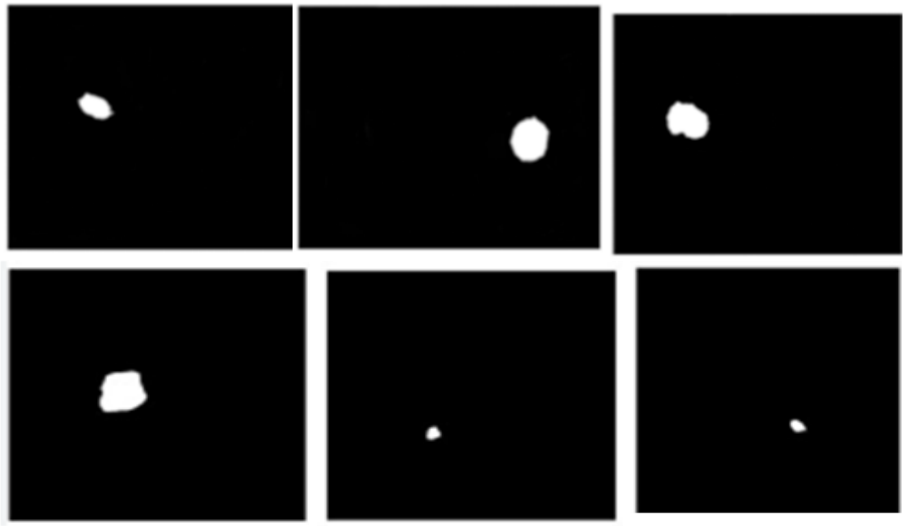

Fig 5: Segmented tumor using ADBN based segmentation

Following preprocessing, the liver is segmented using the ADBN model shown in Figure 5. This segmentation examines the pixels that surround the initial seed points to determine whether they ought to be included in the region.

Journal of Information Systems Engineering and Management
2025, 10(3)
e-ISSN: 2468-4376
https://www.jisem-journal.com/

Research Article

2.5. Feature extraction and lung tumor detection

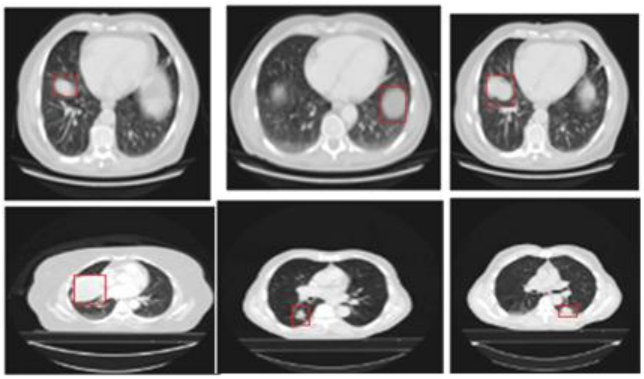

Fig 6: Lung cancer feature extraction using DenseNet-201 model

Figure 6 shows the feature extraction stage utilizing the DenseNet-201 model on the segmentation step's output image. Each image has its unique set of features that help in the detection and classification of cancers.

The graphic above depicts a confusion matrix for lung tumor classification developed by the GWO-EHO model (a hybrid optimization technique that GWO-EHO. The matrix compares actual labels (rows) and expected labels (columns) in three categories: normal, benign, and malignant. Each cell displays the categorization accuracy percentage and related number of cases.

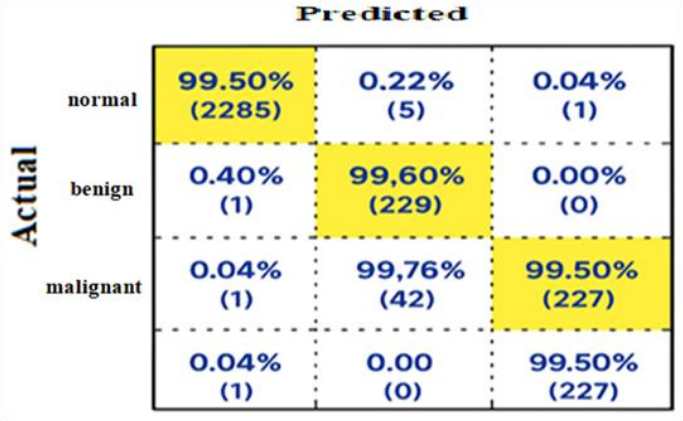

Fig 7: Confusion Matrix for GWO-EHO classification model

The Receiver Operating Characteristic (ROC) curve for a lung tumor classification model that separates the tumors into three classes normal, benign, and malignant is shown in the above Figure 8. The ROC curve is a graphical representation of the model's diagnostic capacity that plots the True Positive Rate (sensitivity) versus the False Positive Rate at various categorization thresholds. In this scenario, a one-vs-rest (OvR) technique was adopted, with unique ROC curves constructed for each class compared to the other two. This result suggested that the GWO-EHO deep learning model is extremely accurate in differentiating between normal lung tissue and lung tumors, whether benign or malignant.

Journal of Information Systems Engineering and Management
2025, 10(3)
e-ISSN: 2468-4376
https://www.jisem-journal.com/

Research Article

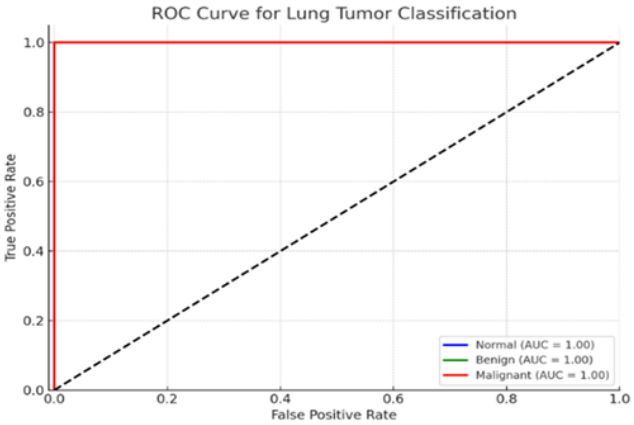

Fig 8: ROC curve for lung cancer classification

Table 2 presents a full comparison of various categorization algorithms, including accuracy, precision, and sensitivity.

Table 2: Comparison of the effectiveness for multiple classification techniques

Reference	Method	Accuracy (%)	Precision (%)	Sensitivity (%)
[20]	K-Nearest Neighbor (KNN)	96	90.1	85.97
[21]	Modified U-Net model	97.98	97.1	97.70
[22]	EfficientNet	99.10	96	98.5
Proposed	GWO-EHO algorithm	99.5	97.3	99.4

CONCLUSION

The proposed methodology effectively enhances lung cancer diagnosis through a comprehensive pipeline involving preprocessing, segmentation, feature extraction, and classification. The application of the AOWMF significantly reduces noise in CT lung images, improving the quality of input data. The use of the ADBN for segmentation enables accurate identification of affected regions, while the DenseNet-201 model ensures robust and detailed feature extraction. Furthermore, the hybrid GWO-EHO classification strategy demonstrates superior performance in classifying lung cancer cases into normal, benign, and malignant categories, achieving high precision and classification accuracy. The proposed GWO-EHO algorithm has an accuracy of 99.5% in that order. For future work, the model can be extended to work with larger and more diverse datasets to enhance its generalizability across different populations and imaging conditions.

REFERENCE

[1] Imran, Muhammad, Bushra Haq, Ersin Elbasi, Ahmet E. Topcu, and Wei Shao. "Transformer Based Hierarchical Model for Non-Small Cell Lung Cancer Detection and Classification." IEEE Access (2024).
[2] Siddiqui, Ebtasam Ahmad, Vijayshri Chaurasia, and Madhu Shandilya. "Detection and classification of lung cancer computed tomography images using a novel improved deep belief network with Gabor filters." Chemometrics and Intelligent Laboratory Systems 235 (2023): 104763.
[3] Avinash, S., K. Manjunath, and S. Senthil Kumar. "An improved image processing analysis for the detection of lung cancer using Gabor filters and watershed segmentation technique." In 2016 International Conference on Inventive Computation Technologies (ICICT), vol. 3, pp. 1-6. IEEE, 2016.
[4] Jena, Sanjukta Rani, Thomas George, and Narain Ponraj. "Texture analysis based feature extraction and classification of lung cancer." In 2019 IEEE International Conference on Electrical, Computer and Communication Technologies (ICECCT), pp. 1-5. IEEE, 2019.
[5] Agarwal, Aman, and Kritik Patni. "Lung cancer detection and classification based on alexnet CNN." In 2021 6th international conference on communication and electronics systems (ICCES), pp. 1390-1397. IEEE, 2021.

[6] Chen, Ying, Yerong Wang, Fei Hu, Longfeng Feng, Taohui Zhou, and Cheng Zheng. "LDNNET: towards robust classification of lung nodule and cancer using lung dense neural network." IEEE Access 9 (2021): 50301-50320.
[7] Da Nóbrega, Raul Victor Medeiros, Solon Alves Peixoto, Suane Pires P. da Silva, and Pedro Pedrosa Rebouças Filho. "Lung nodule classification via deep transfer learning in CT lung images." In 2018 IEEE 31st international symposium on computer-based medical systems (CBMS), pp. 244-249. IEEE, 2018.
[8] Nazir, Imran, Ihsan Ul Haq, Muhammad Mohsin Khan, Muhammad Bilal Qureshi, Hayat Ullah, and Sharjeel Butt. "Efficient pre-processing and segmentation for lung cancer detection using fused CT images." Electronics 11, no. 1 (2021): 34.
[9] Das, Kaushik Pratim, and J. Chandra. "A review on preprocessing techniques for noise reduction in PET-CT images for lung cancer." In Congress on Intelligent Systems: Proceedings of CIS 2021, Volume 2, pp. 455-475. Singapore: Springer Nature Singapore, 2022.
[10] Gainey, Jordan C., Yusen He, Robert Zhu, Stephen S. Baek, Xiaodong Wu, John M. Buatti, Bryan G. Allen, Brian J. Smith, and Yusung Kim. "Predictive power of deep-learning segmentation based prognostication model in non-small cell lung cancer." Frontiers in oncology 13 (2023): 868471.
[11] Finnegan, Robert Neil, Lucia Orlandini, Xiongfei Liao, Jun Yin, Jinyi Lang, Jason Dowling, and Davide Fontanarosa. "Feasibility of using a novel automatic cardiac segmentation algorithm in the clinical routine of lung cancer patients." Plos one 16, no. 1 (2021): e0245364.
[12] Sun, Wenqing, Bin Zheng, and Wei Qian. "Automatic feature learning using multichannel ROI based on deep structured algorithms for computerized lung cancer diagnosis." Computers in biology and medicine 89 (2017): 530-539.
[13] Hussain, Lal, Wajid Aziz, Abdulrahman A. Alshdadi, Malik Sajjad Ahmed Nadeem, Ishtiaq Rasool Khan, and Qurat-Ul-Ain Chaudhry. "Analyzing the dynamics of lung cancer imaging data using refined fuzzy entropy methods by extracting different features." IEEE Access 7 (2019): 64704-64721.
[14] Nanglia, Pankaj, Sumit Kumar, Aparna N. Mahajan, Paramjit Singh, and Davinder Rathee. "A hybrid algorithm for lung cancer classification using SVM and Neural Networks." ICT Express 7, no. 3 (2021): 335-341.
[15] Rodrigues, Murillo B., Raul Victor M. Da Nobrega, Shara Shami A. Alves, Pedro Pedrosa Reboucas Filho, Joao Batista F. Duarte, Arun K. Sangaiah, and Victor Hugo C. De Albuquerque. "Health of things algorithms for malignancy level classification of lung nodules." IEEE Access 6 (2018): 18592-18601.
[16] Mohamed, Tehnan IA, and Absalom E. Ezugwu. "Enhancing lung cancer classification and prediction with deep learning and multi-omics data." IEEE Access (2024).
[17] Chen, Ying, Yerong Wang, Fei Hu, Longfeng Feng, Taohui Zhou, and Cheng Zheng. "LDNNET: towards robust classification of lung nodule and cancer using lung dense neural network." IEEE Access 9 (2021): 50301-50320.
[18] Hoseini, Zeynab, Hesam Varaee, Mahdi Rafieizonooz, and Jang-Ho Jay Kim. "A new enhanced hybrid grey wolf optimizer (GWO) combined with elephant herding optimization (EHO) algorithm for engineering optimization." Journal of Soft Computing in Civil Engineering 6, no. 4 (2022): 1-42.
[19] Sivakumar, Maheswari, and Sundar Chinnasamy. "An efficient combined intelligent system for segmentation and classification of lung cancer computed tomography images." PeerJ Computer Science 10 (2024): e1802.
[20] Taher, F., N. Prakash, A. Shaffie, A. Soliman, and A. El-Baz. "An overview of lung cancer classification algorithms and their performances." IAENG International Journal of Computer Science 48, no. 4 (2021): 1021-1027.
[21] Naseer, Iftikhar, Sheeraz Akram, Tehreem Masood, Muhammad Rashid, and Arfan Jaffar. "Lung cancer classification using modified u-net based lobe segmentation and nodule detection." IEEE Access 11 (2023): 60279-60291.
[22] Raza, Rehan, Fatima Zulfiqar, Muhammad Owais Khan, Muhammad Arif, Atif Alvi, Muhammad Aksam Iftikhar, and Tanvir Alam. "Lung-EffNet: Lung cancer classification using EfficientNet from CT-scan images." Engineering Applications of Artificial Intelligence 126 (2023): 106902.